

## Quantum chemistry of the minimal CdSe clusters

Ping Yang,<sup>1</sup> Sergei Tretiak,<sup>1,2,3</sup> Artëm E. Masunov,<sup>4</sup> and Sergei Ivanov<sup>3,a)</sup><sup>1</sup>Theoretical Division, Los Alamos National Laboratory, Los Alamos, New Mexico 87545, USA<sup>2</sup>Center for Nonlinear Studies (CNLS), Los Alamos National Laboratory, Los Alamos, New Mexico 87545, USA<sup>3</sup>Center for Integrated Nanotechnologies (CINT), Los Alamos National Laboratory, Los Alamos, New Mexico 87545, USA<sup>4</sup>Nanoscience Technology Center (NSTC), University of Central Florida, Florida 32826, USA;

Department of Chemistry, University of Central Florida, Florida 32826, USA;

Department of Physics, University of Central Florida, Florida 32826, USA

(Received 4 June 2008; accepted 7 July 2008; published online 21 August 2008)

Colloidal quantum dots are semiconductor nanocrystals (NCs) which have stimulated a great deal of research and have attracted technical interest in recent years due to their chemical stability and the tunability of photophysical properties. While internal structure of large quantum dots is similar to bulk, their surface structure and passivating role of capping ligands (surfactants) are not fully understood to date. We apply *ab initio* wavefunction methods, density functional theory, and semiempirical approaches to study the passivation effects of substituted phosphine and amine ligands on the minimal cluster Cd<sub>2</sub>Se<sub>2</sub>, which is also used to benchmark different computational methods versus high level *ab initio* techniques. Full geometry optimization of Cd<sub>2</sub>Se<sub>2</sub> at different theory levels and ligand coverage is used to understand the affinities of various ligands and the impact of ligands on cluster structure. Most possible bonding patterns between ligands and surface Cd/Se atoms are considered, including a ligand coordinated to Se atoms. The degree of passivation of Cd and Se atoms (one or two ligands attached to one atom) is also studied. The results suggest that B3LYP/LANL2DZ level of theory is appropriate for the system modeling, whereas frequently used semiempirical methods (such as AM1 and PM3) produce unphysical results. The use of hydrogen atom for modeling of the cluster passivating ligands is found to yield unphysical results as well. Hence, the surface termination of II–VI semiconductor NCs with hydrogen atoms often used in computational models should probably be avoided. Basis set superposition error, zero-point energy, and thermal corrections, as well as solvent effects simulated with polarized continuum model are found to produce minor variations on the ligand binding energies. The effects of Cd–Se complex structure on both the electronic band gap (highest occupied molecular orbital–lowest unoccupied molecular orbital energy difference) and ligand binding energies are systematically examined. The role played by positive charges on ligand binding is also explored. The calculated binding energies for various ligands *L* are found to decrease in the order OPMe<sub>3</sub> > OPH<sub>3</sub> > NH<sub>2</sub>Me ≧ NH<sub>3</sub> ≧ NMe<sub>3</sub> > PMe<sub>3</sub> > PH<sub>3</sub> for neutral clusters and OPMe<sub>3</sub> > OPH<sub>3</sub> > PMe<sub>3</sub> ≧ NMe<sub>3</sub> ≧ NH<sub>2</sub>Me ≧ NH<sub>3</sub> > PH<sub>3</sub> and OPMe<sub>3</sub> > OPH<sub>3</sub> > NH<sub>2</sub>Me ≧ NMe<sub>3</sub> ≧ PMe<sub>3</sub> ≧ NH<sub>3</sub> > PH<sub>3</sub> for single and double ligations of positively charged Cd<sub>2</sub>Se<sub>2</sub><sup>2+</sup> cluster, respectively. © 2008 American Institute of Physics. [DOI: 10.1063/1.2965532]

### I. INTRODUCTION

Colloidal semiconductor nanocrystals (NCs) are ligand-surfactant-stabilized particles of 1–100 nm in size can be placed in the range between molecular compounds and single crystals. They are often referred to as colloidal quantum dots (QDs) for the reason that their fundamental electronic and optical properties are critically size dependent due to the effect of quantum confinement.<sup>1</sup> NCs with high degree of size control can be synthesized by convenient organometallic methods. They are composed of a semiconductor core protected from the surrounding medium with a layer of organic molecules.<sup>2</sup> Unlike traditional organic fluorophores,

NCs have excellent photostability and resistance to photobleaching that make them advantageous for various photophysical applications. The surface ligands, such as trioctylphosphine oxide (TOPO), trioctylphosphine (TOP), alkyl phosphonic and carboxylic acids, various amines, and/or shells of inorganic materials (“core/shell” systems) play a decisive role in stabilizing the NCs in solution and are believed to have a strong effect on the electronic and optical properties of passivated NCs. Among these ligands, TOPO and TOP are historically ligands of choice for II–VI semiconductor NCs due to their optimal bonding to NC surface (these ligands bind strong enough to NC surface to enable size control of NCs and weak enough to ensure NC nucleation and growth). On the other hand, the use of only TOPO/TOP ligands does not allow achieving high quantum yields for these NC systems. For that, the use of primary amines is

<sup>a)</sup>Author to whom correspondence should be addressed. Electronic mail: ivanov@lanl.gov.

required, despite the experimental and theoretical observations that amines appear to bind weaker to II–VI SC NCs compared to phosphine and phosphine oxide ligands, which manifest in decreased quantum yield stability of amine-protected NCs.<sup>3</sup> It was also observed experimentally that the luminescence efficiency of II–VI NCs cannot be restored at full upon the attempts to passivate NC surface for a second time after ligands were dissociated from NC surface. All these experimental results point out to the importance of the surface reconstruction for NC properties. However, little is still known about the NC surface structure to design the synthetic conditions and types of ligands that would address the shortcomings of currently utilized approaches. A recent experimental survey showed that both the type and the quality of surface passivation are very important for such optical properties as, for instance, the optical gain or photoinduced absorption.<sup>3</sup> Experimental studies of CdSe QDs capped by oxygen-coordinating ligand TOPO using NMR,<sup>4</sup> x-ray photoelectron spectroscopy (XPS),<sup>5</sup> and extended x-ray absorption fine structure spectroscopy (EXAFS) (Ref. 6) techniques established that the surface Se atoms are not likely to be passivated, and it appears that surface passivation first and foremost occurs via ligand coordination to surface metal atoms.

In the past few years, tremendous computational and theoretical progress in understanding the unique properties of QDs has been achieved.<sup>6,7</sup> However, the details of surface passivation process are still not clear. In the past, theoretical studies of the unsaturated valences (dangling bonds) on the surface were either left truncated or saturated by hydrogen<sup>8</sup> or oxygen atoms,<sup>9,10</sup> rather than more realistic surfactants. The precise nature of ligands was unspecified, and each ligand was simply being assumed to supply single  $sp^3$ -hybridized orbital that bonds with the Cd atoms.<sup>11</sup> Thus, the effect of NC surface reconstruction has not been properly addressed. For example, based on the simplistic particle-in-a-box approach, the effective-mass approximation (EMA) model and its “ $k \cdot p$ ” generalization fail to encompass the detailed ligand passivation and focus on the modification of the envelope of electron wavefunctions induced by the confinement only.<sup>12</sup> So far, EMA was only applied to ligand-free QDs and results were found to significantly disagree with experimental values.<sup>13</sup> Other studies have been carried out for ligand-free QDs at semiempirical<sup>14</sup> techniques and density functional theory<sup>15</sup> (DFT) utilizing local density approximation or generalized gradient approximation (GGA) models. A ligand potential model has been used to simulate the surface passivation.<sup>10,16,17</sup> However, the arbitrary magnitude of the potential and of the distance between the ligands and the surface atoms can affect the calculated values of the optical band gaps. The electronic properties of CdSe NCs were found to be sensitive to their environment in a study that simulated the environment using self-consistent reaction field and semiempirical pseudopotential methods.<sup>6,18,19</sup> Hydrogen atoms were used as model ligands in semiempirical pseudopotential in order to saturate dangling bonds.<sup>8</sup> A recent QD calculation using effective tight-binding model and a simple model for QD surface reconstruction based on observations of bulk surface relaxations was carried out using

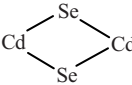
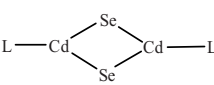
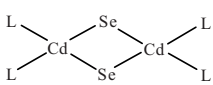
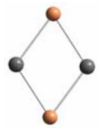
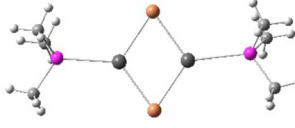
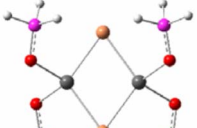
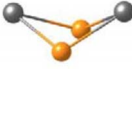
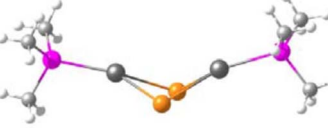
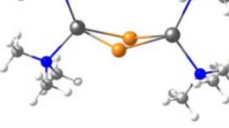
oxygen atoms as passivation ligands to surface Cd.<sup>17</sup> In another study, the dangling bonds on the surface were removed by shifting the energies of the corresponding hybrid orbitals well above the conduction band edge by about 100 eV.<sup>20</sup> The possibility of surface reorganization by partially saturating Se dangling bonds thus has been neglected in previous theoretical investigations. More realistic simulations of the surface reconstruction using first principle methods had been published recently,<sup>16,19,21</sup> and include self-healing and ligand effect of CdSe NCs.

Even though experimental results<sup>2,22</sup> illustrate that the CdSe NCs adopt the wurtzite structure in its interior, the details of interactions between the organic ligands and surface of NC are still not well understood. For a rational control of QD properties, the following fundamental issues need to be addressed: (1) What kinds of surface sites on a NC surface are available for binding with ligands? (2) What is the detailed effect of the ligands on electronic properties of semiconductor clusters, including the highest occupied molecular orbital–lowest unoccupied molecular orbital (HOMO–LUMO) (band) gap? (3) What are the ligand binding energies to NC surfaces? These questions need to be answered by proper computational model for each type of ligand considering the chemical nature and computational cost. In this work, we present a systematic theoretical investigation of these issues by focusing on the minimal cluster  $Cd_2Se_2$  to compare different theoretical methodologies currently available in the standard quantum chemical codes. The use of minimal cluster allows us to determine an appropriate theory level, which would produce results comparable to computationally expensive state-of-the-art *ab initio* wavefunction methods. Such comparisons clearly show glaring inaccuracies inherent to the existing commonly used semiempirical models. Furthermore, our computational results allow us to establish minimal models of surface ligands that suffice to reproduce binding energies and cluster geometries. In the follow up study, we investigate several small CdSe clusters using the formulated computational approaches. This article is organized as follows: The details of our computational approach are presented in Sec. II. In Sec. III we analyze the results of our numerical simulations and rationalize the emerging trends. Finally, we summarize our findings in Sec. IV.

## II. COMPUTATIONAL STRATEGY

*General approach.* In our study, several computational methodologies are compared among each other. Semiempirical methods (AM1, MNDO/d, PM3, and PM5), DFT functionals (including GGA and hybrid functionals), and *ab initio* methods [RHF, MP2, MP4(SDQ), and CCSD] are considered. The coupled-cluster theoretical approach technique serves nowadays as a standard among the most accurate approaches to the exact solution of the many-body problem. Using the bottom-up approach and starting with smallest CdSe cluster,  $Cd_2Se_2$ , we establish a benchmark in terms of most cost-efficient theoretical method which can be used for reliable geometry optimizations, cluster-ligand binding energies estimates, and to ascertain the simplest computational

TABLE I. Examples of typical optimal Cd<sub>2</sub>Se<sub>2</sub> structures.

	 $L = \text{PH}_3, \text{PMe}_3, \text{NH}_3, \text{NH}_2\text{Me}, \text{NMe}_3, \text{OPH}_3, \text{OPMe}_3$	 $L = \text{PH}_3, \text{PMe}_3, \text{NH}_3, \text{NH}_2\text{Me}, \text{NMe}_3, \text{OPH}_3, \text{OPMe}_3$
 Bare Cd <sub>2</sub> Se <sub>2</sub>	 $L = \text{PMe}_3$ (1)	 $L = \text{OPH}_3$ (2)
 Bare Cd <sub>2</sub> Se <sub>2</sub> <sup>2+</sup>	 $L = \text{PMe}_3$ (1)	 $L = \text{NMe}_3$ (2)

models for passivating ligands we can use which would still provide results expandable onto real systems.

**Model clusters.** This work initiates atomistic-level investigation into the nature of interactions between capping ligands and surface atoms of CdSe nanostructures. The minimal neutral Cd<sub>2</sub>Se<sub>2</sub> cluster with 1:1 ratio<sup>23</sup> between Cd and Se atoms was chosen as a model to study chemical bonding between ligands and cluster atoms studied, bare and ligated Cd<sub>2</sub>Se<sub>2</sub> structures are shown in Table I. Even though this small rhomboid shaped cluster is too small to be considered a QD, we believe the cluster is sufficient for benchmark purposes of various theoretical methodologies.

Different degrees of Cd<sub>2</sub>Se<sub>2</sub> cluster passivation with coordinating ligands have been analyzed to investigate their influence on molecular geometries and ligand binding energies. Assuming ideal tetrahedral environment around Cd or Se in NCs, the complexes with no more than two ligands per each Cd and/or Se atom combinations in Cd<sub>2</sub>Se<sub>2</sub> are studied (see Table I). Further in the text, we refer to Cd or Se atoms in Cd<sub>2</sub>Se<sub>2</sub> as “singly passivated” if only one ligand is bound to the atom and “doubly passivated” if two ligands are bound to it, and as “unpassivated” when no ligand is coordinated to the atom.

For initial geometry optimizations of all studied complexes, no symmetry constrains are assumed. Since optimized structures conform very closely to either  $C_{2h}$  (for complexes with singly passivated Cd and/or Se atoms) or  $D_2$  point groups (for complexes with doubly passivated Cd atoms), further calculations are performed under corresponding symmetry restrictions. No imaginary frequencies in IR

spectra of optimized complexes are introduced in case of the symmetry-constrained optimizations, indicating true potential energy minimum structures. Some geometrical parameters of optimized structures are shown in Tables II–V.

**Model ligands.** In order to estimate the effects caused by various ligands, we select the following neutral ligand models: H, NH<sub>3</sub>, NH<sub>2</sub>Me, NMe<sub>3</sub>, PH<sub>3</sub>, PMe<sub>3</sub>, OPH<sub>3</sub>, and OPMe<sub>3</sub>. In the presented row, H atom is the simplest agent to saturate dangling bonds, and its use in calculations works well for organic and silicon systems,<sup>24</sup> but it is unclear if the H atom is an appropriate passivating ligand for CdSe QDs.<sup>25</sup> TOP and TOPO are the most commonly used passivating ligands in the synthesis of colloid QDs. As such, PH<sub>3</sub> and OPH<sub>3</sub> would be the simplest analogs of these two agents, respectively. To validate whether it is acceptable to substitute alkyl groups by H atoms, the methyl substituted ligands, PMe<sub>3</sub> and OPMe<sub>3</sub>, are also studied. Similarly, the simplest models (NH<sub>3</sub> and NH<sub>2</sub>Me) of widely used primary amines (such as hexadecylamine or octylamine) have been investigated as well. To judge the suitability of the model ligands used to approximate the real ligand systems, we use the following two criteria. The first one is the retention of Cd<sub>2</sub>Se<sub>2</sub> cluster connectivity upon the ligation with the model ligand, and the second one is the qualitative convergence of the ligand binding energies to the experimentally observed trends of ligand bonding to a NC. Noteworthy, the Cd<sub>2</sub>Se<sub>2</sub> cluster cannot properly simulate the steric interactions between ligands on a surface. This limitation will be considered by investigating larger QDs to be discussed in the consecutive article.

TABLE II. Optimal geometries of ligand-free Cd<sub>2</sub>Se<sub>2</sub> cluster calculated using different theoretical model chemistries.

Methods	Bond lengths (Å)		HOMO-LUMO gap (eV)	
	Cd–Se	Cd–Cd		
RHF	LANL2DZ	2.590	2.919	7.2
	LANL2DZ**	2.572	2.903	7.3
	SDD	2.596	2.921	7.1
	SDD**	2.576	2.917	7.2
	STO-3G	2.394	2.329	10.0
	STO-3G**	2.301	2.548	9.1
	LANL2MB	2.715	3.280	6.4
B3LYP	LANL2DZ	2.663	2.981	2.9
	LANL2DZ**	2.637	2.966	2.3
	SDD	2.611	2.868	2.2
	SDD**	2.587	2.855	2.3
	STO-3G	2.381	2.234	3.6
	STO-3G**	2.278	2.429	2.9
	LANL2MB	2.782	3.322	1.7
OPBE	LANL2DZ	2.641	2.947	1.3
	LANL2DZ**	2.618	2.938	1.5
	SDD	2.582	2.815	1.3
	SDD**	2.558	2.807	1.4
	STO-3G	2.404	2.272	2.6
	STO-3G**	2.294	2.483	1.9
	LANL2MB	2.765	3.295	0.8
SVWN5	LANL2DZ	2.631	2.891	1.1
	LANL2DZ**	2.606	2.882	1.2
	SDD	2.563	2.746	1.1
	SDD**	2.538	2.735	1.2
	STO-3G	2.341	2.196	2.0
	STO-3G**	2.244	2.373	1.4
	LANL2MB	2.756	3.257	0.6
AM1	2.081	1.968	4.7	
PM3	2.512	3.068	6.5	
PM5	2.914, 2.141	2.179	7.3	

**Quantum chemical methods.** All theoretical quantum chemical calculations were performed using GAUSSIAN03 (G03) package.<sup>26</sup> To determine the optimal method for calculations of Cd<sub>2</sub>Se<sub>2</sub> structures, different basis sets combined with Hartree–Fock, DFT, and highly correlated wavefunction methods have been utilized. We also tested the most widely used semiempirical methods, such as AM1, PM3, and PM5 as coded in the MOPAC package.<sup>27</sup>

DFT has already established itself as a method of choice for NC calculations.<sup>11,19,28</sup> However, no systematic study has been conducted on the appropriate choice of DFT functional for these calculations. In this paper we have tested SVWN5 functional<sup>29</sup> as a typical local spin density approximation (LSDA) functional that includes Slater exchange and VWN 5 local correlation functional. As a representative functional of DFT GGA approach, we use OPBE with OPTX modification of Becke's exchange,<sup>30</sup> whereas hybrid DFT-HF GGA approach is represented by widely used B3LYP functional, which includes a 20% mixture Hartree–Fock exchange, Becke's exchange functional with nonlocal correlation provided by the LYP expression, and VWN functional III for local correlation.<sup>31</sup>

As an alternative to DFT methods, we use *ab initio* methods such as Hartree–Fork,<sup>32</sup> Møller–Plesset second order and fourth order perturbation theory (MP2 and MP4(SDQ))(Ref. 33) and coupled-cluster with singlets and doublets<sup>34</sup> (CCSD) theory to understand the correlation effects on geometries, binding energies, zero-point energies, and Gibbs free energies. Frequency calculations are used to verify that optimized geometries correspond to the local minima. Because no experimental data are available for the studied complexes, we assume that upon systematic introduction of correlation effects in a stepwise manner, high level correlation corrected methods are expected to be increasingly accurate for obtaining realistic geometries and energies. As such, CCSD is being the most accurate method among considered.

For selected systems, basis set superposition errors (BSSE) by means of counterpoise (CP) correction have been analyzed.<sup>35</sup> Zero-point energy corrections and thermal corrections analysis are also conducted using vibrational frequency calculations and thermal analysis in harmonic approximation as coded in GAUSSIAN package of programs.<sup>36</sup> Solvent effects are simulated using IEFPCM polarizable continuum solvation model,<sup>37</sup> as implemented in GAUSSIAN 03.

The following basis sets are tested in our study: minimal basis sets (all-electrons STO-3G and LANL2MB, 18-valence-electrons LANL ECP basis),<sup>38</sup> LANL2DZ double- $\zeta$  18-valence-electrons basis set with LANL ECP;<sup>39</sup> and SDD triple- $\zeta$  18-valence-electrons basis set with Stuttgart/Dresden ECP. Most of these basis sets are also used with additional single set of polarization functions on all atoms.

Ligand static polarizabilities have been estimated using G03 package (keyword POLAR). The polarizabilities were calculated at B3LYP level with 6-311G(d,p), triple- $\zeta$  full electron basis set with one polarization function on all ligand atoms and after the ligand geometry was optimized at B3LYP/LANL2DZ level of theory.

**Ligand binding energies.** The binding energies listed in Tables III and IV are average binding energies per ligand molecule. One of the issues is variation of the stepwise binding energy from the average binding energy. We calculate

$$\overline{BE}_n = \frac{1}{n}(E_{\text{Cd}_2\text{Se}_2L_n} - E_{\text{Cd}_2\text{Se}_2} - nE_L),$$

$$BE_{2L \rightarrow 4L} = E_{\text{Cd}_2\text{Se}_2L_4} - E_{\text{Cd}_2\text{Se}_2L_2} - 2E_L,$$

where  $\overline{BE}_n$  is the average binding energy per ligand in Cd<sub>2</sub>Se<sub>2</sub>L<sub>n</sub> complex;  $BE_{2L \rightarrow 4L}$  is the binding energy per ligand upon the ligation of Cd<sub>2</sub>Se<sub>2</sub>L<sub>2</sub> complex with two extra ligands *L*;  $E_{\text{Cd}_2\text{Se}_2L_n}$  is the potential energy of Cd<sub>2</sub>Se<sub>2</sub>L<sub>n</sub> complex;  $E_{\text{Cd}_2\text{Se}_2}$  is the energy of bare cluster Cd<sub>2</sub>Se<sub>2</sub>;  $E_L$  is the potential energy of ligand *L*, and *n* is the number of ligands in the complex.

### III. RESULTS AND DISCUSSION

**Hydrogen ligand.** Hydrogen atom is the simplest surface terminating ligand and is often used in simulation of a ligation in large clusters.<sup>8</sup> Our geometry optimizations of Cd<sub>2</sub>Se<sub>2</sub> cluster ligated by different number of H atoms resulted in the



TABLE III. Calculated parameters for  $\text{Cd}_2\text{Se}_2(\text{PH}_3)_4$  and  $\text{Cd}_2\text{Se}_2(\text{PMe}_3)_4$  clusters using different theoretical model chemistries. (Binding energies calculated using B3LYP geometries are given in parentheses.)

Methods	Bond lengths (Å)						HOMO-LUMO gap (eV)		$\overline{BE}_2$ (kcal/mol)		
	Cd–Se		Cd–Cd		Cd–L		PH <sub>3</sub>	PMe <sub>3</sub>	PH <sub>3</sub>	PMe <sub>3</sub>	
	PH <sub>3</sub>	PMe <sub>3</sub>	PH <sub>3</sub>	PMe <sub>3</sub>	PH <sub>3</sub>	PMe <sub>3</sub>	PH <sub>3</sub>	PMe <sub>3</sub>	PH <sub>3</sub>	PMe <sub>3</sub>	
RHF	STO-3G	2.433	2.441	2.386	2.388	2.723	2.684	13.1	7.9	–17.8	–21.3
	STO-3G**	2.372	2.368	3.055	3.058	2.242	2.280	11.3	7.9	–31.7	–37.2
	LANL2MB	2.708	2.723	3.390	3.457	3.062	2.941	8.9	9.6	–11.3	–19.0
	LANL2DZ	2.620	2.643	3.074	3.140	2.948	2.835	9.3	9.5	–10.3	–15.8
	LANL2DZ**	2.605	2.638	3.046	3.126	2.930	2.798	7.8	7.1	–8.4	–15.9
	SDD	2.629	2.653	3.066	3.128	2.936	2.833	7.8	7.9	–10.5	–16.1
	SDD**	2.612	2.640	3.051	3.129	2.956	2.811	7.4	7.1	–7.8	–15.1
B3LYP	STO-3G	2.414	2.441	2.257	2.261	2.721	2.638	5.4	3.9	–15.4	–19.5
	STO-3G**	2.379	2.383	3.134	3.140	2.133	2.154	4.8	3.8	–44.3	–50.2
	LANL2MB	2.757	2.769	3.374	3.438	3.091	2.982	3.3	3.7	–9.1	–16.3
	LANL2DZ	2.676	2.697	3.098	3.164	2.982	2.895	3.5	3.9	–9.1	–14.2
	LANL2DZ**	2.653	2.681	3.065	3.146	2.990	2.861	3.3	3.7	–7.0	–13.7
	SDD	2.629	2.653	3.013	3.085	2.864	2.782	3.3	3.9	–10.0	–15.2
	SDD**	2.603	2.634	2.996	3.086	2.878	2.748	3.3	3.6	–7.0	–13.7
OPBE	STO-3G	2.432	2.377	2.300	2.300	2.723	2.706	3.7	2.7	–13.0	–16.4
	STO-3G**	2.379	2.383	3.115	3.131	2.139	2.166	3.2	2.6	–40.1	–45.2
	LANL2MB	2.745	2.757	3.340	3.396	3.102	2.979	2.2	2.7	–6.8	–13.7
	LANL2DZ	2.659	2.678	3.054	3.112	3.043	2.941	2.4	2.9	–6.1	–10.4
	LANL2DZ**	2.633	2.657	3.015	3.088	3.070	2.916	2.3	2.5	–3.6	–9.9
	SDD	2.603	2.623	2.942	3.008	2.850	2.782	2.3	2.7	–7.1	–11.6
	SDD**	2.574	2.602	2.927	3.016	2.852	2.734	2.3	2.4	–3.8	–10.6
SVWN5	STO-3G	2.379	2.428	2.231	2.320	2.508	2.437	3.4	2.9	–25.0	–33.6
	STO-3G**	2.350	2.355	3.123	3.127	2.075	2.102	3.3	2.9	–66.1	–78.8
	LANL2MB	2.727	2.746	3.305	3.387	2.925	2.859	2.4	2.9	–16.3	–26.8
	LANL2DZ	2.654	2.677	3.022	3.098	2.790	2.734	2.5	3.0	–16.2	–24.7
	LANL2DZ**	2.631	2.659	2.992	3.083	2.783	2.708	2.4	2.9	–14.0	–24.3
	SDD	2.590	2.618	2.905	2.985	2.633	2.592	2.4	2.9	–19.5	–28.1
	SDD**	2.564	2.601	2.895	2.996	2.620	2.553	2.5	2.8	–15.8	–27.0
MP2/LANL2DZ	2.612	2.630	2.948	2.970	2.811	2.687	...	...	–12.8 (–13.4)	–21.4 (–24.0)	
MP4(SDQ)/LANL2DZ	2.613	2.634	2.965	2.998	2.826	2.709	...	...	–12.2 (–12.7)	–20.3 (–23.5)	
CCSD/LANL2DZ	2.617	2.634	2.976	3.010	2.834	2.715	...	...	–11.9 (–12.4)	–20.0 (–23.3)	
AM1	2.781	2.731	2.101	2.276	3.318	4.109	5.0	5.4	–20.4	–21.9	
PM3	2.508	2.513	3.653	3.279	2.403	2.791	6.4	6.4	–19.9	–14.1	
PM5		2.681			2.547						
		3.135	3.022	2.319	2.235	2.394	2.469	7.2	7.7	–38.7	–34.0
		2.177	2.270								

formation of either  $\text{H}_x\text{Se}$  or  $\text{H}_y\text{Cd}$  hydrides with complete disruption of Cd–Se bonding. The structural parameters for relaxed structures of fully H-passivated complexes are shown in Fig. 1(a). This type of behavior is typical for all *ab initio* calculations used in this work. As follows from the observed data, we conclude that according to the first criterion outlined above (retention of  $\text{Cd}_2\text{Se}_2$  cluster integrity), H atom is not capable of simulating the real ligand system in passivating CdSe NCs, and it is not considered as a viable passivating ligand further.

*Choice of the basis set for geometry optimizations.* All combinations of DFT functionals and basis sets described

above have been used to optimize the geometry of the bare cluster  $\text{Cd}_2\text{Se}_2$ . Obtained optimization results are presented in Table II. Based on the convergence of DFT results compared to the higher-level methods, LANL2DZ basis set as implemented in G03 is standing out as the best compromise between efficiency and accuracy of performed calculations. No extra polarization functions are included in the further optimization calculations as they do not change the results significantly, while substantially increasing the computational cost. Unless stated otherwise, RHF, B3LYP, OPBE and CCSD methods are used in combination with LANL2DZ basis set in the further study.

TABLE IV. Parameters for  $\text{Cd}_2\text{Se}_2L_n$  ( $n=2$  and 4). Calculated at different levels of theory using LANL2DZ basis set. [The data in parentheses represent  $BE_{2L-4L}$  binding energies (see text).]

Ligand	Geometry parameters (Å)												HOMO-LUMO gap (eV)			$\overline{BE}_2$ (kcal/mol)			
	Cd-Se				Cd-Cd				Cd-L				RHF	B3LYP	OPBE	RHF	B3LYP	OPBE	CCSD
	RHF	B3LYP	OPBE	CCSD	RHF	B3LYP	OPBE	CCSD	RHF	B3LYP	OPBE	CCSD	RHF	B3LYP	OPBE	RHF	B3LYP	OPBE	CCSD
$\text{PH}_3$ (1)	2.599	2.660	2.643	2.600	3.026	3.052	3.009	2.938	2.817	2.910	2.956	2.748	8.8	3.1	2.2	-14.9	-12.5	-9.4	-17.3
$\text{PH}_3$ (2)	2.620	2.676	2.659	2.617	3.074	3.098	3.054	2.976	2.948	2.982	3.043	2.834	9.3	3.5	2.4	-10.3 (-5.6)*	-9.1 (-5.7)	-6.1 (-2.9)	-11.9 (-7.4)
$\text{PMe}_3$ (1)	2.609	2.665	2.649	2.603	3.060	3.079	3.036	2.960	2.718	2.811	2.831	2.652	8.8	3.5	2.5	-23.0	-19.2	-15.9	-26.3
$\text{PMe}_3$ (2)	2.643	2.697	2.678	2.634	3.140	3.164	3.112	3.010	2.835	2.895	2.941	2.715	9.5	3.5	2.9	-15.8 (-8.7)	-14.2 (-9.2)	-10.4 (-4.8)	-20.0 (-14.4)
$\text{NH}_3$ (1)	2.604	2.664	2.648	2.604	3.021	3.053	3.015	2.928	2.361	2.401	2.427	2.362	8.7	3.2	2.3	-26.0	-25.1	-21.2	-28.3
$\text{NH}_3$ (2)	2.640	2.708	2.692	2.632	3.084	3.124	3.094	2.967	2.428	2.432	2.463	2.409	8.6	3.7	2.8	-20.1 (-14.2)	-20.5 (-15.9)	-16.5 (-11.8)	-22.3 (-16.2)
$\text{NH}_2\text{Me}$ (1)	2.605	2.666	2.649	2.604	3.024	3.056	3.018	2.930	2.353	2.396	2.427	2.343	8.8	3.3	2.4	-26.9	-25.8	-21.1	-30.1
$\text{NH}_2\text{Me}$ (2)	2.641	2.705	2.694	...	3.096	3.131	3.105	...	2.430	2.434	2.474	...	8.9	3.8	3.0	-20.5 (-14.2)	-20.8 (-15.8)	-16.2 (-11.2)	...
$\text{NMe}_3$ (1)	2.605	2.667	2.650	2.603	3.026	3.056	3.024	2.923	2.364	2.403	2.450	2.330	9.3	3.5	2.6	-26.2	-24.9	-18.6	-34.4
$\text{NMe}_3$ (2)	2.644	2.702	2.686	2.635	3.121	3.141	3.138	2.960	2.478	2.483	2.592	2.398	9.8	4.0	2.8	-19.0 (-11.8)	-19.3 (-13.6)	-16.5 (-5.6)	-28.2 (-22.9)
$\text{OPH}_3$ (1)	2.576 2.691	2.623 2.748	2.613 2.728	2.571 2.670	3.112	3.098	3.052	2.946	2.154	2.232	2.254	2.225	8.9	3.1	2.0	-39.3	-32.1	-24.2	-36.3
$\text{OPH}_3$ (2)	2.696	2.739	2.718	2.661	3.204	3.228	3.197	3.014	2.247	2.270	2.311	2.279	9.2	3.5	2.4	-31.6 (-23.8)	-27.3 (-22.6)	-19.4 (-14.5)	-30.0 (-23.6)
$\text{OPMe}_3$ (1)	2.577 2.685	2.632 2.734	2.629 2.698	2.580 2.654	3.107	3.132	3.080	2.979	2.162	2.214	2.255	2.198	9.2	3.6	2.5	-44.3	-37.3	-28.1	-42.9
$\text{OPMe}_3$ (2)	2.688	2.728	2.708	...	3.248	3.245	3.214	...	2.253	2.298	2.351	...	9.6	4.0	2.8	-33.6 (-23.0)	-29.6 (-21.9)	-20.2 (-12.2)	...

TABLE V. Calculated Gibbs free energy (kcal/mol) per each ligand in  $\text{Cd}_2\text{Se}_2L_n$  ( $n=2$  and 4) cluster at B3LYP/LANL2DZ level of theory.

Ligand	$\Delta G_1^0$ per ligand	$\Delta G_2^0$ per ligand
$\text{PH}_3$ (1)	-6.2	...
$\text{PH}_3$ (2)	-0.8	4.7
$\text{PMe}_3$ (1)	-14.2	...
$\text{PMe}_3$ (2)	-4.8	4.5
$\text{NH}_3$ (1)	-16.1	...
$\text{NH}_3$ (2)	-9.6	-3.0
$\text{NH}_2\text{Me}$ (1)	-12.9	...
$\text{NH}_2\text{Me}$ (2)	-9.1	-5.3
$\text{NMe}_3$ (1)	-15.7	...
$\text{NMe}_3$ (2)	-6.3	3.2
$\text{OPH}_3$ (1)	-27.7	...
$\text{OPH}_3$ (2)	-20.0	-12.3
$\text{OPMe}_3$ (1)	-32.5	...
$\text{OPMe}_3$ (2)	-21.5	-10.6

*Geometric structures.* Various initial geometries of ligated complexes have been considered, including both Cd and Se atoms coordinating different number of model ligands. Geometry optimization results reveal that regardless of the number and the initial positions of the ligands, no ligand remains bound to Se atoms after structure optimization. The initial guesses included the ligands bound only to Se, to both Se and Cd, and only Cd atoms. During optimization, the ligands either completely dissociate from Se atom or move onto adjacent Cd atom if the latter was not four coordinated initially. The optimization results in only two possible stable types of complexes remained: those with one or two ligands bonded to Cd atom [e.g., see Fig. 1(b)]. These results rule out the possibility of ligand models utilized in this work to bind to Se atoms of neutral  $\text{Cd}_2\text{Se}_2$ . This conclusion also agrees with experimental findings,<sup>23,40</sup> suggesting that ligands almost exclusively coordinate to  $\text{Cd}^{2+}$  ions during the growth process of NCs. After optimizations by all used computational methods, the cluster  $\text{Cd}_2\text{Se}_2$  remains planar. In the case of singly passivated structures, shown on Table I, the Cd-bound atoms of ligands (N, O, and P atoms) are in the same plane as the core cluster  $\text{Cd}_2\text{Se}_2$ . For doubly passivated complexes, Cd atoms possess tetrahedral coordination, and ligands are located above and below the plane of  $\text{Cd}_2\text{Se}_2$  core.

Comparison between the geometries of bare and ligated complexes of  $\text{Cd}_2\text{Se}_2$  (Tables II–IV) reveals the expected stretch in Cd–Se bond upon ligation. The binding of the first ligand,  $\text{NH}_3$ ,  $\text{PH}_3$ , or  $\text{OPH}_3$  to each Cd atom causes slight shortening of the Cd–Se bond by 0.01–0.02 Å, as more electron density is transferred to Cd–Se framework from nucleophilic ligand, the fact that is verified by Natural Population analysis. Addition of the second ligand onto each Cd atom causes the Cd–Se bond to stretch because of the stronger steric repulsion from the ligands. The more realistic ligands of  $\text{NMe}_3$ ,  $\text{PMe}_3$ , or  $\text{OPMe}_3$  affect the Cd–Se bonds in the same way (see Table IV). One can notice that the Cd–Se bond lengths change less than 2% for all methods and basis sets. Unlike Cd–Se bond length, value of which is relatively

uniform regardless of the method used, Cd–L bond lengths vary by a larger magnitude depending on the method. DFT GGA calculations give the longest ligand binding distance, followed by the hybrid B3LYP, then RHF, and finally by LSDA level of theory, which gives the shortest ligand binding distance for all basis sets. This observation follows the general DFT trend, with LSDA usually overestimating the binding energy in molecular structures, a well-known drawback of LSDA.

It should be noted that structures of all neutral  $\text{Cd}_2\text{Se}_2$  complexes have another distinct minimum at 30–60 kcal above the global minimum, where  $\text{CdSe}_2\text{Cd}$  plane puckers and two selenium atoms in  $\text{Cd}_2\text{Se}_2$  form Se–Se bond in the range of 2.6–2.9 Å. When the complex acquires +2 charge, this local minimum becomes the global one due to the depletion of electron density on Se atoms (see below).

Semiempirical methods are computationally inexpensive and could be used to study large complexes. However, geometry optimization results obtained with any of the semiempirical methods with conventional parametrization were found to be inconsistent with DFT and post-HF results. The geometries given by the methods were often unphysical. For example, AM1 predicts either complete ligand dissociation from the cluster or its binding to the cluster through the hydrogen atoms bridges [see Fig. 1(c)]. In addition, Cd···Cd separation was found to be too small (1.968 Å) to be considered a viable result. PM3 predicts both Cd and Se atoms to be singly ligated. PM5 leads to  $\text{Cd}_2\text{Se}_2$  dissociation into a pair of monomers with two short Cd–Se bond distances (2.177 Å) and two long ones (3.135 Å). These results contradict both DFT and the high level wavefunction methods (such as MP4 and CCSD). Therefore, common semiempirical methods with default parametrization for Cd and Se are not reliable to study CdSe QD systems.

*DFT functional and basis set dependence of the calculated geometries, band gaps, and binding energies.* Geometric and electronic band-gap data for the bare cluster  $\text{Cd}_2\text{Se}_2$ , obtained using various combinations of methods and basis sets, are presented in Table II. The data demonstrate that these properties are both method and basis set dependent. When using the same basis sets, the predicted Cd–Se bond lengths are found to decrease within 0.02 Å in the following order: B3LYP > OPBE > SVWN5 > RHF. The results from HF, MP2, MP4(SDQ), and CCSD calculations show the bond-length dependence on the degree of electronic correlation. Going from HF to CCSD, Cd–L bond lengths change nonmonotonously, with typical overcorrection for MP2.

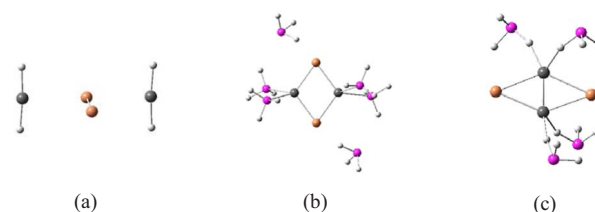


FIG. 1. (Color online) Examples of unphysical optimized structures of  $\text{Cd}_2\text{Se}_2L_n$ . (a) Each Cd atom is passivated with two H atoms; (b) each Se (Cd) is capped with one (two) ligand(s); and (c) each Cd is capped with two ligands after AM1 optimization.

From MP2 to MP4 to CCSD, the results gradually converge towards the HF results. Evidently, due to the error cancellation from the overestimation of electrostatic interaction and the neglect of electron correlation within HF method framework, RHF results are in close agreement with more accurate CCSD method.

The minimal STO-3G basis set underestimates Cd–Se bond length and Cd··Cd separation in both bare and ligated Cd<sub>2</sub>Se<sub>2</sub> clusters regardless of the method option (Tables II and III). Typically, STO-3G gives the highest binding energy by overestimating the  $\pi$ -acceptor characteristics of electropositive elements. In contrast, the combination of the minimal basis set with Los Alamos effective core potential (ECP) in LANL2MB leads to the overestimation of the bond lengths by  $\sim 0.12$  Å and higher Cd–L bond energies. The double- $\zeta$  LANL2DZ gives rise to about 0.06 Å longer Cd–Se bond distances than triple- $\zeta$  SDD basis sets, when used with B3LYP, OPBE, and SVWN5 DFT functionals. Apparently, split valence basis sets enable better description of both electron-nuclear attraction and electron correlation. Although addition of *d*- and *f*-orbital polarization functions is expected to be important, the calculations demonstrate that polarization functions do not significantly affect the cluster geometries (decrease all Cd–Se bonds by 0.02 Å), while they slow down the calculations by a factor of  $\sim 3$ . The geometric and energetic properties of the clusters, fully passivated with PH<sub>3</sub> or PMe<sub>3</sub> ligands (see Table III), demonstrate the basis set dependence similar to the bare cluster. Overall, the use of double split valence ECP basis set LANL2DZ without polarization is adequate for the study of Cd–Se-ligand complex geometry relaxation.

We do not recommend the use of the minimal basis sets STO-3G, STO-3G\*\*, and LANL2MB due to unphysical geometries and unreasonably high binding energies produced. The ECP with double- $\zeta$  quality valence basis set (LANL2DZ) is found to predict bond lengths in bare cluster with performance comparable to more complete, triple- $\zeta$  basis set with Stuttgart pseudopotential, SDD. Additional polarization functions added on all atoms change Cd-ligand bond lengths by less than 3% and binding energies by less than 1 kcal/mol. The use of triple- $\zeta$  basis set with four sets of polarization functions, 6-311G(3df,3pd), on all *ligand* atoms has also been tested and has shown to produce the 10%–20% increase in binding energies of phosphine ligands. Finally, the CP correction<sup>35</sup> (CP) for BSSE at B3LYP/LANL2DZ level uniformly decreases the metal-ligand binding energies by 8%–10%. Based on the tests above, we conclude that LANL2DZ basis provides best compromise between the computational costs and accuracy, and we recommend its use for further calculations. These observations suggest that with one exception of highly polarizable lone pair on the phosphorus atom, the intra-atomic polarization does not contribute to the calculated properties significantly, compared to interatomic electron delocalization even for the small clusters. Hence, improvements in the valence basis functions, suggested recently,<sup>41,42</sup> may further increase the accuracy.

The predicted HOMO-LUMO gap values in Cd<sub>2</sub>Se<sub>2</sub> are strongly dependent on the choice of the calculation method

and weakly dependent on basis sets. Within DFT frame, LSDA and GGA functionals result in the small gap values (1.1 and 1.7 eV, respectively). The application of hybrid B3LYP functional results in the HOMO-LUMO gap value of 2.2 eV. In contrast to DFT, the Hartree–Fock approach significantly increases the gap to 7.7 eV. Comparing the HOMO-LUMO gaps in Tables II and III, in general, we observed that ligation of bare Cd<sub>2</sub>Se<sub>2</sub> cluster leads to the expected widening the HOMO-LUMO gap by about 2 eV for the wave function methods and by about 1 eV for the density functional approach, since the ligands would stabilize the energies of orbitals corresponding to unfilled bonds of the bare cluster.

Analysis of changes in ligand binding energies, shown in Table III, indicates their dependence on both computational functional and type of basis set used. The LSDA functional, SVWN5, gives the highest binding energy and the shortest bond distance, whereas OPBE functional predicts the weakest bonding interaction with the longest metal-ligand bond lengths. The bonding energies given by hybrid functional, B3LYP, fall in between the results given by LSDA and GGA functionals and are reasonably close to the results of CCSD. The minimal basis sets STO-3G and STO-3G\*\* yield unreasonably high binding energies (up to  $-78.8$  kcal/mol), while the addition of polarization functions to LANL2DZ and SDD have little effects on the corresponding binding energies.

Finally, solvent effects can also be responsible for inaccuracies in geometries and energy calculations in studied complexes. To account for solvent influence on ligand interactions with Cd<sub>2</sub>Se<sub>2</sub> complex, we applied IEFPCM implicit solvation model to calculate metal-ligand binding energies in the selected clusters. As expected, the solvent produced uniform weakening of the coordination bonds (by  $\sim 10\%$  in the chloroform solution).

*Binding energies and thermodynamics.* Relative binding energies for the first and second passivating ligands on each Cd atom are found to be method independent. The results for B3LYP/LANL2DZ theory level are given in Table IV and can be summarized in the following two rows of decreasing ligand binding strengths. Upon binding of the first or second ligand to the metal ion in bare cluster, energies of binding decrease in the following order of ligands: OPMe<sub>3</sub> > OPH<sub>3</sub> > NH<sub>2</sub>Me  $\geq$  NH<sub>3</sub>  $\geq$  NMe<sub>3</sub> > PMe<sub>3</sub> > PH<sub>3</sub>. These results correlate with nucleophilicity decrease from phosphine oxides to amines to phosphines. Strong nucleophilicity of phosphine oxides can be attributed to a significantly negative charge on oxygen ( $\sim -1e$ ), while the weaker nucleophilicity of PH<sub>3</sub> is expected due to the lack of electron-donating methyl groups. This effect is manifested in stronger metal-ligand bonds between Cd and NMe<sub>3</sub>, PMe<sub>3</sub>, or OPMe<sub>3</sub> ligands compared to the corresponding bonds between Cd and NH<sub>3</sub>, PH<sub>3</sub>, or OPH<sub>3</sub>. The stretch of Cd–Se bonds in the complexes with methylated ligands is larger than that in complexes with non-methylated ones. The second ligand also elongates the Cd–L bonds and thus decreases the binding energy per ligand (shown in parentheses on Table IV). It should be mentioned that the ligation of each Cd atom in Cd<sub>2</sub>Se<sub>2</sub> with single OPH<sub>3</sub> breaks the symmetry of the complex by making two inversion-equivalent Cd–Se bonds longer compared to the



TABLE VI. Structural parameters for charged  $\text{Cd}_2\text{Se}_2L_n^{2+}$  clusters ( $n=2,4$ ) calculated using B3LYP/LANL2DZ level of theory and static polarizabilities  $P$  for corresponding individual ligands, calculated using B3LYP/6-311G(d, p) level of theory.

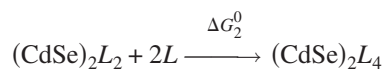
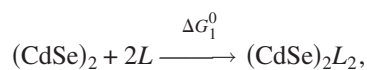
Ligand	Cd–Se $\text{Cd}_2\text{Se}_2L_n^{2+}$	Cd–L <sup>a</sup> $\text{Cd}_2\text{Se}_2L_n^{2+}$	CdSe <sub>2</sub> Cd dihedral angle (°)	Se–Se $\text{Cd}_2\text{Se}_2L_n^{2+}$	Se···Se $\text{Cd}_2\text{Se}_2L_n$	$\overline{BE}_2$ (kcal/mol) in $\text{Cd}_2\text{Se}_2L_n^{2+}$	$P$ (Bohr <sup>3</sup> )
Cd <sub>2</sub> Se <sub>2</sub>	2.740	···	116.7	2.899	4.321	···	···
PH <sub>3</sub> (1)	2.730	2.661	123.2	2.810	4.356	–55.4	24.0
PH <sub>3</sub> (2)	2.762	2.750	134.1	2.758	4.363	–41.7	24.0
PMe <sub>3</sub> (1)	2.742	2.630	125.8	2.785	4.350	–77.9	60.1
PMe <sub>3</sub> (2)	2.780	2.710	143.7	2.726	4.368	–56.2	60.1
NH <sub>3</sub> (1)	2.725	2.250	124.0	2.820	4.367	–69.1	8.7
NH <sub>3</sub> (2)	2.763	2.318	137.9	2.767	4.426	–56.1	8.7
NH <sub>2</sub> Me (1)	2.727	2.243	123.5	2.811	4.368	–73.3	20.0
NH <sub>2</sub> Me (2)	2.766	2.312	140.3	2.758	4.412	–58.2	20.0
NMe <sub>3</sub> (1)	2.733	2.242	125.0	2.806	4.370	–76.0	42.8
NMe <sub>3</sub> (2)	2.777	2.326	146.4	2.751	4.397	–58.0	42.8
OPH <sub>3</sub> (1)	2.727	2.053	120.5	2.813	4.389	–89.2	23.6
OPH <sub>3</sub> (2)	2.768	2.144	122.0	2.751	4.426	–70.1	23.6
OPMe <sub>3</sub> (1)	2.701	2.023	122.1	2.925	4.361	–105.5	56.5
OPMe <sub>3</sub> (2)	2.794	2.131	122.2	2.724	4.387	–80.9	56.5

<sup>a</sup>Average over two types of symmetry-equivalent bonds in  $\text{Cd}_2\text{Se}_2L_4^{2+}$ .

other two bonds (Table IV). The H atoms in phosphine form hydrogen-bonding alike interactions with Se atoms causing two Cd–Se bonds become slightly stretched. Not surprisingly, similar effects are observed for phosphine oxide ligand, in both singly and fully passivated complexes.

The obtained data show that  $BE$  is equal to  $BE_{1,n}$  for every ligand within absolute error of 0.2 kcal/mol. The binding energies decrease from the first ligand to the last one. The variation of  $BE_1$  and  $BE_n$  from the average binding energy is within 4.9 kcal/mol. As a consequence, the difference between the binding energies for the first ligand molecule and the last one could be as large as 10 kcal/mol. Normally,  $BE_1$  is higher than  $BE_n$ , since subsequently added ligands always encounter more steric interactions with the previously bound ligands. Although the last ligand molecule binds to the cluster with the smallest binding energy, this binding is still a thermodynamically preferred process.

Free energy corrections to the total energies of selected complexes have been calculated using vibrational frequency analysis to estimate Gibbs free energy of ligand binding to bare CdSe complexes. The results are summarized in Table V. We found that Gibbs free energy per ligand is negative for all complexes considered, confirming that the ligand coordination is a spontaneous process. However, if the stepwise process is considered,



for  $L=\text{PH}_3$ ,  $\text{PMe}_3$ , and  $\text{NMe}_3$   $\Delta G_1^0$  is negative while  $\Delta G_2^0$  is positive (even though overall  $\Delta G_1^0 + \Delta G_2^0$  is negative). This indicates that each Cd atom in the cluster prefers to remain singly passivated by the ligands. On the contrary, in case of  $\text{NH}_3$ ,  $\text{NH}_2\text{Me}$ ,  $\text{OPH}_3$  and  $\text{OPMe}_3$  the binding of second ligand stabilizes the complexes even further. As we pointed out for cluster  $\text{Cd}_2\text{Se}_2$ , the steric interactions between ligands

can largely be avoided due to the open structure of  $\text{Cd}_2\text{Se}_2$  in three-dimensional space. The ligand binding energies are expected to be reduced for ligands bound to a semiconductor crystal plane (and, therefore, constrained to a limited space) due to increased influence of steric interactions.

*Charge Effects.* Some experimental evidence seems to indicate that semiconductor NCs might possess positive surface charges depending on the synthetic technique used. To gain an insight into the difference between neutral and surface-charged QDs, we have performed calculations on dicationic passivated complexes of  $\text{Cd}_2\text{Se}_2^{2+}$ . The typical structures of charged complexes are presented in Table I and results of geometry optimizations and binding energy calculations are summarized in Table VI and Fig. 2. Although, the charge per atom in such small complexes is significantly higher than that in known semiconductor NCs, and, therefore, the former cannot be considered the realistic models of the latter, we expect that the revealed trends will be useful in our future studies of larger models of semiconductor QDs. The main difference between neutral and positively charged complexes is comprised of a covalent Se–Se bond formation, leading to the puckering of  $\text{Cd}_2\text{Se}_2$  plane ( $\text{CdSe}_2\text{Cd}$  dihedral angle becomes less than  $180^\circ$ ), shortening of Cd–L bond, and significant, two to fourfold increase in the metal-ligand binding energy. From both Mulliken population analysis and natural population analysis<sup>43</sup> it follows that in positively charged complexes effective charge on Cd atoms does not change significantly compared to the neutral case, whereas negative charge on Se atoms decreased by  $\sim 0.5e$  independently on the type of the passivating ligand. Apparently, removal of electrons from the complex effectively depletes the electron density on selenium lone pair thereby leading to the structures with covalent Se–Se bonding becoming lower in energy compared to the structure of neutral  $\text{Cd}_2\text{Se}_2L_n$  complexes. The length of this Se–Se bond was found to strongly correlate with the value of the electric dipole polarizability of the binding ligand (Table VI). Compared to the Se–Se bond

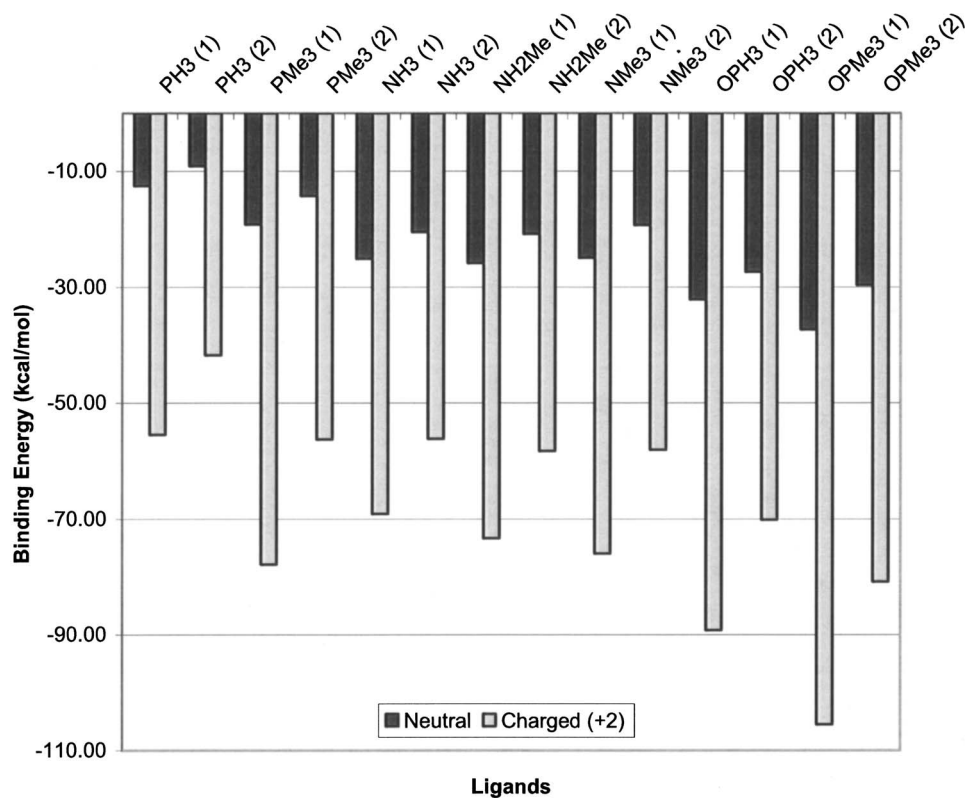


FIG. 2. Summary of calculated average binding energies per ligand for neutral and positively charged complexes  $\text{Cd}_2\text{Se}_2L_n$  ( $n=2$  and  $4$ ) at B3LYP/LANL2DZ level of theory.

distance of 2.899 Å in bare  $\text{Cd}_2\text{Se}_2^{2+}$ , ligand coordination leads to this distance decrease indicating that electron-deficient Se atoms in  $\text{Cd}_2\text{Se}_2^{2+}$  framework form stronger Se–Se bond when more electron density is available from the coordinating ligand. The Se–Se bond length is also found to be inversely proportional to Cd–Se distance in dicationic complexes. In contrast to interatomic bonding, the  $\text{CdSe}_2\text{Cd}$  dihedral angle is found to be insensitive to ligand electron-donating abilities but rather is a function of ligand steric extent (Table VI). In all complexes of type  $\text{Cd}_2\text{Se}_2L_2^{2+}$  this angle changes in the narrow range of  $120^\circ$ – $125^\circ$ , whereas in complexes  $\text{Cd}_2\text{Se}_2L_4^{2+}$ , this angle is in the range of  $134^\circ$ – $146^\circ$  with the largest values observed for the bulkiest  $\text{NMe}_3$  and  $\text{PMe}_3$  ligands. Positive charges on the complexes also lead to slight increase in cadmium electrophilicity and, consequently, shortens Cd–L bonds. The binding energies for the charged clusters listed in Table VI can be arranged in two similar descending orders:  $\text{OPMe}_3 > \text{OPH}_3 > \text{PMe}_3 \geq \text{NMe}_3 \geq \text{NH}_2\text{Me} \geq \text{NH}_3 > \text{PH}_3$  (when only one ligand is binding to one cadmium ion in  $\text{Cd}_2\text{Se}_2^{2+}$ ) and  $\text{OPMe}_3 > \text{OPH}_3 > \text{NH}_2\text{Me} \geq \text{NMe}_3 \geq \text{PMe}_3 \geq \text{NH}_3 > \text{PH}_3$  (when second ligand binds to the same cadmium ion in  $\text{Cd}_2\text{Se}_2^{2+}$ ). Phosphine oxide ligand still demonstrates the strongest binding, but ammonia now binds weaker than the phosphine compared to binding to the neutral  $\text{Cd}_2\text{Se}_2$  complex. One would expect that the ligand polarizability  $P$  should correlate with the energy of its binding to  $\text{Cd}_2\text{Se}_2$  complex. However, we do not observe such correlation in either case of neutral or dicationic complexes. It is likely that multiple factors (such as ligand steric extent, its electronic properties, the size of its coordinating orbitals, etc.) contribute to the ligand binding energy and no single factor is significantly dominating to reveal the expected correlation.

Generally, the charges on the cluster slightly stretch the Cd–Se bond lengths in both bare and passivated clusters due to the depletion of electron density in the complex framework. In contrast, the metal-ligand distances get shorter by  $\sim 0.1$  Å due to the increased electrophilicity of Cd atom. Overall, the positive charge on the complex leads to the expected dramatic increase in ligand binding, especially for phosphine ligands.

#### IV. CONCLUSIONS

Using various theoretical model chemistries, we have studied computationally the effect of different ligands on the structure and energetics of  $\text{Cd}_2\text{Se}_2$  complex, structural precursor to CdSe QDs. Compared to the higher order electron correlated methods (CCSD and MP4), the geometry of complexes studied is most *cost effectively* predicted at RHF/LANL2DZ level, while the energetics is better reproduced at B3LYP/LANL2DZ level. The use of minimal basis sets (both full electron and combined with effective core potential) produce significantly deteriorated results compared to the double- $\zeta$  basis sets and should be avoided together with semiempirical methods that are also unable to reproduce the results of more accurate DFT and correlated *ab initio* wavefunction methods. BSSE correction, zero-point energy and thermal corrections, polarization functions in the basis set, and solvent effect within the polarizable continuum model result in small (less than 10%) changes in the ligand binding energies and do not alter the revealed trends in complex geometries and ligand binding energies. These corrections are likely to be unnecessary for accurate geometry calculations. The use of triple- $\zeta$  basis set can have a larger (up to 30%) effect on geometry and complex energetics, but still does not

change the order of the binding energies. These results can serve as justification for the use of B3LYP/LANL2DZ theory level for calculations of larger clusters. During the preparation of this manuscript, new experimental results<sup>44</sup> were reported along the same line of ligand binding. The reported binding free energies for alkylamines around 10 kcal/mol are in good agreement with our calculations using model systems.

We found that H atom, often used in cluster simulations, tends to disrupt Cd–Se bonding topology and cannot represent the effects of more complex ligands for the small clusters studied. Consequently, one should avoid using simple H atom capping when modeling realistic QD structure. It is desirable to use larger groups which reproduce the binding chemistry as elaborated in this study. It was also found that Se atoms do not bind to any of ligands considered, even in positively charged complexes, whereas cadmium can coordinate up to two ligands. Since Se atoms in studied Cd<sub>2</sub>Se<sub>2</sub> complex are highly coordinatively unsaturated, their inability to form any bond with considered nucleophilic ligands allows us to speculate that no such bonds will be formed on the surface of actual CdSe NCs, as Se atoms in these NCs are even less electrophilic than in Cd<sub>2</sub>Se<sub>2</sub> complex. Although the coordination of one or two ligands to single Cd atom in Cd<sub>2</sub>Se<sub>2</sub> is found to be thermodynamically favorable process. Entropic effects significantly increase Gibbs free energy of this process, and for several ligands (PH<sub>3</sub>, PMe<sub>3</sub>, and NMe<sub>3</sub>)  $\Delta G_2^0$  becomes even positive. These results provide a number of insights on the possible surface structures of ligand-passivated colloidal QDs and serve as the first approximation to the subsequent studies taking additional steric effects into account.

We also found that the positive charge on the cluster leads to the formation of covalent Se–Se bond and significantly stronger binding of ligands to the metal atom. The order of the binding strength changes from OPMe<sub>3</sub> > OPH<sub>3</sub> > NH<sub>2</sub>Me  $\cong$  NH<sub>3</sub>  $\cong$  NMe<sub>3</sub> > PMe<sub>3</sub> > PH<sub>3</sub> for neutral clusters (for both first and second ligations) to OPMe<sub>3</sub> > OPH<sub>3</sub> > PMe<sub>3</sub>  $\cong$  NMe<sub>3</sub>  $\cong$  NH<sub>2</sub>Me  $\cong$  NH<sub>3</sub> > PH<sub>3</sub> and OPMe<sub>3</sub> > OPH<sub>3</sub> > NH<sub>2</sub>Me  $\cong$  NMe<sub>3</sub>  $\cong$  PMe<sub>3</sub>  $\cong$  NH<sub>3</sub> > PH<sub>3</sub> for single and double ligations of positively charged Cd<sub>2</sub>Se<sub>2</sub><sup>2+</sup> cluster, respectively. This provides detailed computational indication for the chemical differences between neutral and charged QDs. Investigations of larger and more realistic models of colloidal QDs are under way and will be reported in the following article.

## ACKNOWLEDGMENTS

We would like to thank Dr. Enrique Batista and Dr. Richard L. Martin for their expertise and helpful discussions. This contribution is supported in part by LANL LDRD program and CNLS LANL student visitor program. LANL is operated by Los Alamos National Security, LLC, for the National Nuclear Security Administration of the U.S. Department of Energy under Contract No. DE-AC52-06NA25396.

<sup>1</sup>W. J. Parak, D. Gerion, T. Pellegrino, D. Zanchet, C. Micheel, S. C. Williams, R. Boudreau, M. A. Le Gros, C. A. Larabell, and A. P. Alivisatos, *Nanotechnology* **14**, R15 (2003); X. Michalet, F. Pinaud, T. D.

- Lacoste, M. Dahan, M. P. Bruchez, A. P. Alivisatos, and S. Weiss, *Single Mol.* **2**, 261 (2001).
- <sup>2</sup>C. B. Murray, D. J. Norris, and M. G. Bawendi, *J. Am. Chem. Soc.* **115**, 8706 (1993).
- <sup>3</sup>A. V. Malko, A. A. Mikhailovsky, M. A. Petruska, J. A. Hollingsworth, and V. I. Klimov, *J. Phys. Chem. B* **108**, 5250 (2004).
- <sup>4</sup>L. R. Becerra, C. B. Murray, G. G. Griffin, and M. G. Bawendi, *J. Chem. Phys.* **100**, 3297 (1994).
- <sup>5</sup>J. E. B. Katari, V. L. Colven, and A. P. Alivisatos, *J. Phys. Chem.* **98**, 4109 (1994).
- <sup>6</sup>L. Manna, L. W. Wang, R. Cingolani, and A. P. Alivisatos, *J. Phys. Chem. B* **109**, 6183 (2005).
- <sup>7</sup>J. Y. Rempel, B. L. Trout, M. G. Bawendi, and K. F. Jensen, *J. Phys. Chem. B* **110**, 18007 (2006); G. Neshet, L. Kronik, and J. R. Chelikowsky, *Phys. Rev. B* **71**, 035344 (2005); W. Wang, S. Banerjee, S. Jia, M. L. Steigerwald, and I. P. Herman, *Chem. Mater.* **19**, 2573 (2007).
- <sup>8</sup>A. Puzder, A. J. Williamson, F. Gygi, and G. Galli, *Phys. Rev. Lett.* **91**, 037401 (2003).
- <sup>9</sup>N. A. Hill and K. B. Whaley, *J. Chem. Phys.* **100**, 2831 (1994).
- <sup>10</sup>K. Leung and K. B. Whaley, *J. Chem. Phys.* **110**, 11012 (1999).
- <sup>11</sup>A. Puzder, A. J. Williamson, F. Gygi, and G. Galli, *Phys. Rev. Lett.* **92**, 217401 (2004).
- <sup>12</sup>H. Haug and S. W. Kock, *Quantum Theory of the Optical and Electronic Properties of Semiconductors* (World Scientific, Singapore, 1993).
- <sup>13</sup>A. Zunger, *Phys. Status Solidi B* **224**, 727 (2001); M. Califano and A. Zunger, *Abstr. Pap. - Am. Chem. Soc.* **225**, U452 (2003); L. W. Wang and A. Zunger, *Phys. Rev. B* **53**, 9579 (1996); A. Zunger, *Phys. Status Solidi B* **224**, 727 (2001).
- <sup>14</sup>V. S. Gurin, *J. Phys.: Condens. Matter* **6**, 8691 (1994); J. Robles, O. Mayorga, T. Lee, and D. Diaz, *Nanostruct. Mater.* **11**, 283 (1999); K. Toth and T. A. Pakkanen, *J. Comput. Chem.* **14**, 667 (1993).
- <sup>15</sup>J. M. Matxain, J. E. Fowler, and J. M. Ugalde, *Phys. Rev. A* **61**, 053201 (2000); J. O. Joswig, M. Springborg, and G. Seifert, *J. Phys. Chem. B* **104**, 2617 (2000).
- <sup>16</sup>C. Troparevsky, L. Kronik, and J. R. Chelikowsky, *J. Chem. Phys.* **114**, 943 (2001); **119**, 2284 (2003); L. W. Wang and A. Zunger, *Phys. Rev. B* **53**, 9579 (1996).
- <sup>17</sup>S. Pokrant and K. B. Whaley, *Eur. Phys. J. D* **6**, 255 (1999).
- <sup>18</sup>T. Rabini, B. Hetényi, and B. Berne, *J. Chem. Phys.* **110**, 5355 (1999); J. T. Hu, L. W. Wang, L. S. Li, W. D. Yang, and A. P. Alivisatos, *J. Phys. Chem. B* **106**, 2447 (2002); J. R. Sachleben, V. Colvin, L. Emsley, E. W. Wooten, and A. P. Alivisatos, *ibid.* **102**, 10117 (1998); D. J. Milliron, A. P. Alivisatos, C. Pitois, C. Edder, and J. M. J. Frechet, *Adv. Mater. (Weinheim, Ger.)* **15**, 58 (2003).
- <sup>19</sup>A. Puzder, A. J. Williamson, N. Zaitseva, G. Galli, G. Manna, and A. P. Alivisatos, *Nano Lett.* **4**, 2361 (2004).
- <sup>20</sup>P. C. Chen and K. B. Whaley, *Phys. Rev. B* **70**, 45311 (2004).
- <sup>21</sup>L. Pizzagalli, G. Galli, J. E. Klepeis, and F. Gygi, *Phys. Rev. B* **63**, 165324 (2001).
- <sup>22</sup>J. J. Shiang, A. V. Kadavanich, R. K. Grubbs, and A. P. Alivisatos, *J. Phys. Chem.* **99**, 17417 (1995).
- <sup>23</sup>L. Manna, E. Scher, and A. P. Alivisatos, *J. Am. Chem. Soc.* **122**, 12700 (2000); Z. A. Peng and X. Peng, *ibid.* **123**, 1389 (2001); **124**, 3343 (2002).
- <sup>24</sup>S. Kilina, S. Tretiak, *Adv. Funct. Mater.* **17**, 3405 (2007).
- <sup>25</sup>M. Lopez del Puerto, M. L. Tiago, and J. R. Chelikowski, *Phys. Rev. Lett.* **97**, 096401 (2006).
- <sup>26</sup>M. J. Frisch, G. W. Trucks, H. B. Schlegel *et al.*, GAUSSIAN 03, Gaussian Inc., Wallingford, CT, 2004.
- <sup>27</sup>J. J. P. Stewart, MOPAC 2002, Fujitsu Limited, Tokyo, Japan, 2002.
- <sup>28</sup>M. C. Troparevsky, L. Kronik, and J. R. Chelikowsky, *J. Chem. Phys.* **119**, 2284 (2003); J. R. Chelikowsky, L. Kronik, and I. Vasiliev, *J. Phys.: Condens. Matter* **15**, 1517 (2003); K. Eichkorn and R. Ahlrichs, *Chem. Phys. Lett.* **288**, 235 (1998).
- <sup>29</sup>S. H. Vosko, L. Wilk, and M. Nusair, *Can. J. Phys.* **58**, 1200 (1980); J. P. Perdew and Y. Wang, *Phys. Rev. B* **45**, 13244 (1992); W. Kohn and L. J. Sham, *Phys. Rev.* **140**, A1133 (1965).
- <sup>30</sup>J. P. Perdew, K. Burke, and M. Ernzerhof, *Phys. Rev. Lett.* **77**, 3865 (1996); J. P. Perdew, K. Burke, and Y. Wang, *Phys. Rev. B* **54**, 13244 (1996).
- <sup>31</sup>A. D. Becke, *J. Chem. Phys.* **98**, 5648 (1993); C. Lee, W. Yang, and R. G. Parr, *Phys. Rev. B* **37**, 785 (1988); B. Mihlich, A. Savin, H. Stoll, and H. Preuss, *Chem. Phys. Lett.* **157**, 200 (1989).
- <sup>32</sup>C. C. J. Roothan, *Rev. Mod. Phys.* **23**, 69 (1951); J. A. Pople and R. K.

- Nesbet, *J. Chem. Phys.* **22**, 571 (1954); R. McWeeny and G. Dierksen, *ibid.* **49**, 4852 (1968).
- <sup>33</sup>R. Krishnan and J. A. Pople, *Int. J. Quantum Chem.* **14**, 91 (1978); S. Seabo and J. Almollof, *Chem. Phys. Lett.* **154**, 83 (1989); M. Head-Gordon, J. A. Pople, and M. J. Frisch, *ibid.* **153**, 503 (1988).
- <sup>34</sup>J. Cizek, *Adv. Chem. Phys.* **14**, 35 (1969); G. D. Purvis and R. J. Bartlett, *J. Chem. Phys.* **76**, 1910 (1982); G. E. Scuseria and H. F. Schaefer III, *ibid.* **90**, 3700 (1989); G. E. Scuseria, C. L. Janssen, and H. F. Schaefer III, *ibid.* **89**, 7382 (1988).
- <sup>35</sup>S. Simon, M. Duran, and J. J. Dannenberg, *J. Chem. Phys.* **105**, 11024 (1996); S. F. Boys and F. Bernardi, *Mol. Phys.* **19**, 553 (1970).
- <sup>36</sup>D. A. McQuarrie, *Statistical Thermodynamics* (Harper and Row, New York, 1973).
- <sup>37</sup>M. T. Cancès, B. Mennucci, and J. Tomasi, *J. Chem. Phys.* **107**, 3032 (1997); B. Mennucci and J. Tomasi, *ibid.* **106**, 5151 (1997).
- <sup>38</sup>P. J. Hay and W. R. Wadt, *J. Chem. Phys.* **82**, 270 (1985); W. R. Wadt and P. J. Hay, *ibid.* **82**, 284 (1985).
- <sup>39</sup>T. H. Dunning, Jr. and P. J. Hay, in *Modern Theoretical Chemistry*, edited by H. F. Schaefer III (Plenum, New York, 1976), Vol. 3, p. 1; P. J. Hay and W. R. Wadt, *J. Chem. Phys.* **82**, 299 (1985); P. Fuentealba, H. Preuss, and H. Stoll, *Chem. Phys. Lett.* **89**, 418 (1989).
- <sup>40</sup>W. W. Yu, Y. A. Wang, and X. G. Peng, *Chem. Mater.* **15**, 4300 (2003).
- <sup>41</sup>P. J. Hay and W. R. Wadt, *J. Chem. Phys.* **82**, 299 (1985).
- <sup>42</sup>L. E. Roy, P. J. Hay, and R. L. Martin, *J. Chem. Theory Comput.* **4**(7), 1029 (2008).
- <sup>43</sup>F. Weinhold and J. P. Foster, *J. Am. Chem. Soc.* **102**, 7211 (1980); J. E. Carpenter and F. Weinhold, *J. Mol. Struct.: THEOCHEM* **169**, 41 (1988).
- <sup>44</sup>X. Li, D. Copenhaver, C. Sichmeller, and X. Peng, *J. Am. Chem. Soc.* **130**, 5726 (2008).